Continuous wavelet transform analysis of quantum systems with rational potentials

1997 J. Phys. A: Math. Gen. 30 4709

(http://iopscience.iop.org/0305-4470/30/13/022)

J. Phys. A: Math. Gen. **30** (1997) 4709–4729. Printed in the UK PII: S0305-4470(97)78776-6

Continuous wavelet transform analysis of quantum systems with rational potentials

Carlos R Handy† and Romain Murenzi‡

† Department of Physics, Clark Atlanta University, Atlanta, GA 30314, USA

‡ Center for Theoretical Studies of Physical Systems, Clark Atlanta University, Atlanta, GA 30314, USA

Received 17 October 1996, in final form 27 February 1997

Abstract. Given a one-dimensional Sturm–Liouville Schrödinger problem with rational polynomial potential, we can generate the continuous wavelet transform (CWT) for its discrete states, thereby permitting the systematic multiscale reconstruction of the corresponding bound-state wavefunction. A key component in this is the use of properly dilated (a) and translated (b) moments, $\mu_{b,a}(p)$, which readily transform the configuration space Hamiltonian into a finite set of dynamically coupled, linear, first-order differential equations in the dilation-related variable, $\gamma \equiv \frac{1}{2a^2}$:

$$\partial_\gamma \mu_{b,\gamma}(i) = \sum_{j=0}^{m_s} \mathcal{M}_{i,j}[E, b, \gamma]\mu_{b,\gamma}(j) \qquad 0 \leqslant i \leqslant m_s.$$

The infinite scale problem $a = \infty$ ($\gamma = 0$) is readily solved through moment quantization methods and used to generate the $\mu_{b,a}(p)$ moments at all scales. We demonstrate the essentials through the rational fraction potential, $V(x) = \frac{gx^6}{1+\lambda x^2}$, and the $\frac{1}{r}$ Coulomb potential.

0. Overview

Over the last 10 years, wavelet transform analysis has become a powerful tool in the analysis and synthesis of signals and images (Chui 1992). Its main contribution is the definition of a systematic process for identifying, extracting, and reconstructing the multiscale features of a signal through simultaneous time and frequency localization.

Until the recent works by Handy and Murenzi (1996, 1997; HM), the incorporation of wavelet theory into quantum mechanics has depended, almost exclusively, on variational methods. Exceptions to this are the earlier works by Plantevin (1992) on wavelet transform analysis for noninteracting quantum systems, and Paul's (1984) specialized wavelet-coherent state analysis for the one-dimensional harmonic oscillator and Coulomb potentials.

Working within an extended space of properly translated and scaled moments, $\mu_{b,\gamma}(p) = \int \mathrm{d}x\, x^p \exp(-\gamma x^2)\Psi(x+b)$ (for the *Mexican hat* wavelet case, where the scale parameter is defined by $a = \frac{1}{\sqrt{2\gamma}}$), HM have been able to transform the Schrödinger equation, for rational fraction potentials, into a theoretically exact, finite set of dynamically coupled, linear, differential moment equations

$$\partial_\gamma \mu_{b,\gamma}(i) = \sum_{j=0}^{m_s} \mathcal{M}_{i,j}[E, b, \gamma]\mu_{b,\gamma}(j) \qquad 0 \leqslant i,\ j \leqslant m_s \tag{0.1}$$

where the $\mathcal{M}_{i,j}$ coefficients and m_s are dependent on the nature of the potential function. Given the appropriate initial information (for $\gamma = 0$), the solution to these equations

0305-4470/97/134709+21$19.50

readily yields the wavelet transform for the unknown discrete state, which in turn (through various inversion or reconstruction methods) allows us to generate the desired wavefunction configuration, Ψ_E. The only essential ingredient in solving these equations is knowledge of the infinite scale properties, at $a = \infty$ or $\gamma = 0$, of the discrete state desired ($\mu_{b,0}(p)$ and E). This information is readily provided through moment quantization (MQ) techniques.

MQ refers to transforming the configuration space Schrödinger equation, $\mathcal{H}_x\Psi(x) = E\Psi(x)$, into a moment equation (ME), $\nu(p) = \sum_{i=0}^{m_s} C_{p,i}[E]\nu(p+i)$, where $\nu(p) \equiv \mu_{0,0}(p)$, and quantizing within such a representation. The ME is equivalent to generating the power series expansion coefficients for the Fourier transform of the configuration space wavefunction solution ($\Psi_E(x) \rightarrow \tilde{\Psi}_E(k)$). Clearly, depending on the nature of the potential function, the associated Fourier representation will involve a differential operator of arbitrarily high order ($\tilde{\mathcal{H}}_k$). In terms of the ME represention, this involves an increased number of independent (initialization or *missing moment*) variables, than the usual *two* associated with second-order differential operators in configuration space.

For the last 16 years, the development of MQ methods has received much attention by several independent groups. One of the earlier formulations by Blankenbecler *et al* (1980) quantized the ME representation of the Schrödinger equation by imposing constraints derived from asymptotic information about the (physical) power moments ($\mathrm{Lim}_{p\rightarrow\infty}\,\nu(p)$). Refinements by Killingbeck *et al* (1985), attempted to simplify this procedure, as well as incorporate regular perturbation theory methods (in this regard, refer also to Fernandez and Ogilvie 1993). The incorporation of perturbation theory within the ME representation has been particularly effective, particularly as pursued in subsequent, multidimensional, investigations by Witwit (1995).

Paralleling these developments are the works by Handy and Bessis (1985; HB), and Handy *et al* (1988) who made unprecedented use of the *moment problem* (Shohat and Tamarkin 1963) nature of the ME representation, as applied to bosonic ground states. Their method, *the eigenvalue moment method* (EMM), introduced linear programming to quantum physics, in a significant way, and also produced one of the simplest theories for generating converging lower and upper bounds to the ground-state energy (which can also be extended to excited states, provided certain empirical assumptions are made, Handy and Lee (1991)). Also, because of its nonperturbative nature, the EMM approach is sensitive to singular-perturbation/strong-coupling type Hamiltonians, and has easily solved important multidimensional problems when compared with more sophisticated approaches (Handy *et al* 1988). In contrast to the asymptotic methods by Blankenbecler *et al* (1980), the EMM approach requires no asymptotic information about the moments (which, in general, can be difficult to obtain). Instead, it focuses on the importance of the *missing moment* structure of the ME representation.

Another related approach is the *Rayleigh–Ritz missing moment* analysis recently developed by Handy (1996). It may be easier to implement, for larger-dimensioned systems, than the EMM analysis.

Any one of the QM approaches cited can be used in implementing the methods developed here. However, the latter two highlight the essential role that the missing moments play in the incorporation of continuous wavelet analysis in quantum mechanics.

In this work we apply the HM formalism, in some detail, to two rational polynomial potential problems: $V(x) = \frac{gx^6}{1+\lambda x^2}$, and the $\frac{1}{r}$ Coulomb potential. Previous works by HM primarily focus on implementing their moment-wavelet formalism in the context of the quartic anharmonic oscillator potential problem.

For simplicity, we limit our analysis to the ground-state case only. Handy and Murenzi (1996) have shown how to extend the analysis to excited states.

Our formalism applies to a broad class of wavelets. The exclusive appearance of the *Mexican hat* wavelet in this work is only for convenience. In general, the methods developed here apply to any wavelet of the form $\partial_x^i e^{Q(x)}$, $i \geqslant 1$, provided $Q(x)$ is a polynomial, and $\mathrm{Lim}_{|x|\to\infty}[\partial_x^i e^{Q(x)}] = 0$.

1. Continuous-wavelet analysis

An important aspect of wavelet analysis is the notion of a *frame*. It was introduced by Duffin and Schaefer (1952) and used by Daubechies *et al* (1986), and Daubechies (1990) for canonical and affine coherent states.

A family, $\{\psi_j\}_{j\in J}$, of vectors in Hilbert space, $\mathcal{H}$, is called a *frame* if for any $f \in \mathcal{H}$ there exist two constants $A > 0$ and $0 < B < \infty$, such that

$$A\|f\|^2 \leqslant \sum_{j\in J} |\langle\psi_j|f\rangle|^2 \leqslant B\|f\|^2. \tag{1.1}$$

The frame is said to be tight if $A = B$.

Consider the operator $T : \mathcal{H} \to l^2(J)$, defined by $Tf = \{\langle\psi_j|f\rangle\}_{j\in J}$. The operator $D = T^*T$, where T^* is the adjoint operator of T, is invertible and the family

$$\tilde{\psi}_j = (T^*T)^{-1}\psi_j = \frac{2}{A+B}\sum_{k=0}^{\infty}\left(\mathbf{1} - \frac{2D}{A+B}\right)^k \psi_j \tag{1.2}$$

defines the *dual frame* of ψ_j, with corresponding bounds $B^{-1} \leqslant A^{-1} < \infty$.

An important reconstruction formula is

$$f(x) = \sum_{j\in J}\langle\psi_j|f\rangle\tilde{\psi}_j(x) \tag{1.3a}$$

or

$$f(x) = \sum_{j\in J}\langle\tilde{\psi}_j|f\rangle\psi_j(x). \tag{1.3b}$$

Using only the first term in the expansion in equation (1.2), one gets $\tilde{\psi}_{j\,\mathrm{approx}} = \frac{2}{A+B}\psi_j$, resulting in

$$f(x) \approx \frac{2}{A+B}\sum_{j\in J}\langle\psi_j|f\rangle\psi_j(x). \tag{1.4}$$

If the frame is tight, $A = B$, one has $\tilde{\psi}_j = \frac{1}{A}\psi_j$ giving us the exact expression

$$f(x) = \frac{1}{A}\sum_{j\in J}\langle\psi_j|f\rangle\psi_j(x). \tag{1.5}$$

A continuous-wavelet transform requires the selection of a wavelet function, $\omega(x)$, satisfying $\int_{-\infty}^{\infty}\frac{|\hat{\omega}(k)|^2}{|k|}\,\mathrm{d}k < +\infty$, where $\hat{\omega}(k)$ is the Fourier transform (Grossman and Morlet 1984). In addition, we adopt the unit normalization, $\int|\omega(x)|^2 = 1$, utilized by Daubechies (1992) in her dyadic reconstruction formula, given below. One of the more popular wavelet functions is the *Mexican hat*, corresponding to

$$\omega(x) = -\mathcal{N}\partial_x^2\exp(-\tfrac{1}{2}x^2) = \mathcal{N}(1-x^2)\exp(-\tfrac{1}{2}x^2)$$

where $\mathcal{N} = \frac{2}{\sqrt{3}}\pi^{-\frac{1}{4}}$. We shall use this wavelet throughout this work.

The wavelet transform of a one-dimensional signal (wavefunction), $\Psi(x)$, is given by

$$W\Psi(a,b) \equiv \sqrt{a^{-1}} \int \omega\left(\frac{(x-b)}{a}\right)\Psi(x)\,\mathrm{d}x \tag{1.6}$$

where $a > 0$ and b define the scale and translation parameters, respectively.

The recovery of the wavefunction is possible through the use of the relations in equations (1.3*a*) and (1.3*b*):

$$\Psi(x) = \sum_{m,n} \langle \omega_{m,n}(x) | \Psi(x) \rangle \tilde{\omega}_{m,n}(x) \tag{1.7a}$$

or

$$\Psi(x) = \sum_{m,n} \langle \tilde{\omega}_{m,n}(x) | \Psi(x) \rangle \omega_{m,n}(x) \tag{1.7b}$$

where $\omega_{m,n}(x) = a_0^{-m/2}\omega(\frac{x - nb_0a_0^m}{a_0^m})$ define a frame (for arbitrary integers m and n), $\tilde{\omega}_{m,n}(x)$ is its dual frame.

As previously noted, if the frame is *tight* then $\tilde{\omega}_{m,n}(x) = \frac{2}{A+B}\omega_{m,n}(x)$, where $\frac{A}{B} = 1$. If the frame is not tight, $\frac{A}{B} \neq 1$, then there are two possibilities (Daubechies 1990, 1992). The first is to compute the dual frame. For this case, if the frame consists of wavelets (dilations and translations of one mother wavelet, $\omega(x)$), then the dual must be computed for each translation, $\tilde{\omega}_{0,n}$. Although, in principle, this entails the calculation of an infinite number of functions, in practice only a finite number are used. Despite this, there are some special wavelets, $\omega(x)$, and b_0 parameter values, for which even though the $\omega_{m,n}(x)$ are not close to defining a tight frame, nevertheless all the $\tilde{\omega}_{m,n}(x)$ are dilated versions of one function (Daubechies 1992, Frazier *et al* 1988).

The second possibility applies to non-tight *snug* frames for which $\frac{A}{B} \approx 1$. In this case, one may take the first term in the defining series expansion for $\tilde{\omega}_{m,n}(x)$, as in equation (1.4). The resulting approximation yields the reconstruction formula (for the case $a_0 = 2$, $b_0 = 1$) (Daubechies 1991)

$$\Psi(x) \approx \frac{2}{A+B}\sum_{m,n}\omega_{m,n}\frac{1}{\sqrt{2^m}}\omega\left(\frac{(x-n2^m)}{2^m}\right) \tag{1.8}$$

where $\omega_{m,n} \equiv W\Psi(2^m, n2^m)$, and $A + B = 6.819$ (*for the Mexican hat case*).

The reconstruction formula in equation (1.8) is approximating the wavefunction through a superposition of localized oscillating structures. The wavefunction is being approximated in the L^2 norm. Through the EMM discussed in the following section, we will be able to generate a finite number of the $\omega_{m,n}$ coefficients, thereby enabling the approximate reconstruction of the wavefunction.

We stress once more that our principal objective is to show how EMM theory can be used to generate the $\omega_{m,n}$ coefficients. There are many possible wavelet-reconstruction formulae, some involving Gaussians (Cho *et al* 1993) as opposed to the Mexican hat wavelets in equation (1.8). We only utilize equation (1.8) as an example of how to utilize the generated wavelet coefficients in the reconstruction of the wavefunction. Also, the method can be extended to excited states (Handy and Murenzi 1996).

2. Generating the $\omega_{m,n}$ through the EMM

From the preceding discussion, the Mexican hat wavelet transform for the wavefunction is given by (after a translation change of variables):

$$W\Psi(a,b) = \mathcal{N}\sqrt{a^{-1}} \int_{-\infty}^{+\infty} \Psi(b+x)[1-(x/a)^2]\exp(-\tfrac{1}{2}(x/a)^2)\,\mathrm{d}x \tag{2.1}$$

or (defining $\gamma \equiv \frac{1}{2a^2}$)

$$W\Psi(a,b) = \mathcal{N}(2\gamma)^{\frac{1}{4}}[\mu_{b,\gamma}(0) - 2\gamma\mu_{b,\gamma}(2)] \tag{2.2}$$

where

$$\mu_{b,\gamma}(p) \equiv \int_{-\infty}^{+\infty} x^p \Psi(b+x)\exp(-\gamma x^2)\,\mathrm{d}x \qquad p \geqslant 0 \tag{2.3}$$

are the moments of the measure $\Phi_{b,\gamma}(x) \equiv \Psi(b+x)\exp(-\gamma x^2)$.

The moments satisfy the following differential equation with respect to the $\gamma > 0$ variable:

$$\partial_\gamma \mu_{b,\gamma}(p) = -\mu_{b,\gamma}(p+2). \tag{2.4}$$

For all one-dimensional Schrödinger Hamiltonians with rational fraction potentials (as well as many other types of potentials which can be converted into rational fraction form after a suitable change of variables), all of the moments become linearly dependent on the first $1+m_s$ moments (referred to as *missing moments*), where m_s is problem dependent:

$$\mu_{b,\gamma}(p) = \sum_{j=0}^{m_s} M_{E,b,\gamma}(p,j)\mu_{b,\gamma}(j). \tag{2.5}$$

The energy, E, dependent coefficients $M_{E,b,\gamma}(p,j)$ are numerically or algebraically determinable, and must satisfy $M_{E,b,\gamma}(i,j) = \delta_{i,j}$, for $0 \leqslant i,\ j \leqslant m_s$ (Handy and Bessis 1985, Handy *et al* 1988).

Inserting equation (2.5) into equation (2.4) yields a closed set of $(1+m_s)$-coupled, first-order, linear differential equations

$$\partial_\gamma \mu_{b,\gamma}(i) = -\sum_{j=0}^{m_s} M_{E,b,\gamma}(i+2,j)\mu_{b,\gamma}(j) \qquad \text{for } 0 \leqslant i \leqslant m_s. \tag{2.6}$$

For arbitrary b, given the physical energy and starting missing moment values $\{\mu_{b,0}(i) | 0 \leqslant i \leqslant m_s\}$ one can numerically integrate equation (2.6) and proceed to determine the wavelet transform (equation (2.2)). Facilitating this is the relation:

$$\mu_{b,0}(p) = \int_{-\infty}^{+\infty} x^p \Psi(b+x)\,\mathrm{d}x = \int_{-\infty}^{+\infty} (x-b)^p \Psi(x)\,\mathrm{d}x \tag{2.7}$$

or (expanding)

$$\mu_{b,0}(p) = \sum_{q=0}^{p} \binom{p}{q} (-b)^{p-q} \mu_{0,0}(q). \tag{2.8}$$

The physical values for the energy, E, and $\mu_{0,0}(q) \equiv \int_{-\infty}^{+\infty} x^q \Psi(x)$ moments, for $0 \leqslant q \leqslant m_s$, are determined by the EMM (discussed in the following section). In practice, for each pair of values $(a = 2^m,\ b = n2^m)$ at each point $b = n2^m$ we integrate equation (2.6) up to $\gamma = \frac{1}{2}a^{-2} = \frac{1}{2}2^{-2m}$, which then allows us to generate the wavelet transform coefficients $\omega_{m,n}$.

An important observation is that the asymptotic behaviour of the $\mu_{b,\gamma}(p)$ moments, with respect to $\gamma \to \infty$, determines the wavefunction:

$$\mathrm{Lim}_{\gamma\to+\infty}\,\mu_{b,\gamma}(p) = \left(\frac{1}{\sqrt{\gamma}}\right)^{(p+1)} \theta(p/2)\Psi(b) \qquad p = \text{even} \tag{2.9}$$

where $\theta(\rho) = \int_{-\infty}^{+\infty} y^{2\rho}\exp(-y^2)\,\mathrm{d}y$. For $p = 0, 2$, we have $\theta(0) = \sqrt{\pi}$ and $\theta(1) = \sqrt{\pi}/2$. As will be clarified in the following section, an implicit normalization is assumed in the implementation of the EMM quantization. Our numerical comparisons between the wavelet-reconstructed wavefunction and the actual wavefunction (obtained from direct integration of the Schrödinger equation) will assume $\Psi(0)$ to have the value generated through equation (2.9) (approximated by a sufficiently large γ value).

3. A rational fraction potential

We now consider the case of the rational fraction potential problem

$$-\partial_x^2\Psi(x) + \frac{gx^6}{1+\lambda x^2}\Psi(x) = E\Psi(x). \tag{3.1}$$

Let $\Phi_{b,\gamma}(x) \equiv \exp(-\gamma x^2)\Psi(b+x)$, or $\Psi(b+x) = \exp(\gamma x^2)\Phi_{b,\gamma}(x)$. The ensuing equation for $\Phi_{b,\gamma}$ is

$$\left[-\left[\frac{\mathrm{d}^2}{\mathrm{d}x^2} + 4\gamma x\frac{\mathrm{d}}{\mathrm{d}x} + 2\gamma + 4\gamma^2x^2\right] + \left[\frac{g(x+b)^6}{1+\lambda(x+b)^2}\right]\right]\Phi_{b,\gamma}(x) = E\Phi_{b,\gamma}(x). \tag{3.2}$$

Multiplying both sides by $x^p(1+\lambda(x+b)^2)$ leads to a moment equation of sixth order since all of the moments,

$$\mu_{b,\gamma}(p) = \int_{-\infty}^{\infty}\mathrm{d}x\,x^p\exp(-\gamma x^2)\Psi(x+b)$$

for $p \geqslant 6$, are linearly dependent on the first six *missing moments*, $\{\mu_{b,\gamma}(i)|0 \leqslant i \leqslant 5\}$:

$$\begin{aligned}\mu_{b,\gamma}(p+6) = {} & -6b\mu_{b,\gamma}(p+5) + \left[4\gamma^2\frac{\lambda}{g} - 15b^2\right]\mu_{b,\gamma}(p+4)\\ & + \left[8\frac{\lambda}{g}b\gamma^2 - 20b^3\right]\mu_{b,\gamma}(p+3)\\ & + g^{-1}[4\gamma^2(1+\lambda b^2) - 4\gamma\lambda(p+\tfrac{5}{2}) - 15gb^4 + E\lambda]\mu_{b,\gamma}(p+2)\\ & + g^{-1}[-2\lambda\gamma b(6+4p) - 6gb^5 + 2\lambda bE]\mu_{b,\gamma}(p+1)\\ & + g^{-1}[(1+\lambda b^2)(E-\gamma(2+4p)) + \lambda(p+2)(p+1) - gb^6]\mu_{b,\gamma}(p)\\ & + 2\lambda bg^{-1}p(p+1)\mu_{b,\gamma}(p-1) + g^{-1}(1+\lambda b^2)p(p-1)\mu_{b,\gamma}(p-2)\end{aligned} \tag{3.3}$$

and

$$\mu_{b,\gamma}(p) = \sum_{i=0}^{m_s=5} M_{E,b,\gamma}(p,i)\mu_{b,\gamma}(i) \tag{3.4a}$$

with

$$M_{E,b,\gamma}(i,j) = \delta_{i,j} \qquad \text{for } 0 \leqslant i,\ j \leqslant 5. \tag{3.4b}$$

The $M_{E,b,\gamma}(p,i)$ coefficients satisfy the same moment equation relation given above, with respect to the p index. They are generated either numerically or algebraically, through the initialization conditions given in equation (3.4*b*).

The relation (from equation (2.6))

$$\frac{\partial}{\partial\gamma}\begin{pmatrix}\mu_{b,\gamma}(0)\\ \mu_{b,\gamma}(1)\\ \mu_{b,\gamma}(2)\\ \mu_{b,\gamma}(3)\\ \mu_{b,\gamma}(4)\\ \mu_{b,\gamma}(5)\end{pmatrix} = -\begin{pmatrix}\mu_{b,\gamma}(2)\\ \mu_{b,\gamma}(3)\\ \mu_{b,\gamma}(4)\\ \mu_{b,\gamma}(5)\\ \mu_{b,\gamma}(6)\\ \mu_{b,\gamma}(7)\end{pmatrix} \tag{3.5}$$

now becomes (upon substituting equation (3.4*a*))

$$\frac{\partial}{\partial\gamma}\begin{pmatrix}\mu_{b,\gamma}(0)\\ \mu_{b,\gamma}(1)\\ \mu_{b,\gamma}(2)\\ \mu_{b,\gamma}(3)\\ \mu_{b,\gamma}(4)\\ \mu_{b,\gamma}(5)\end{pmatrix} = \begin{pmatrix}0 & 0 & -1 & 0 & 0 & 0\\ 0 & 0 & 0 & -1 & 0 & 0\\ 0 & 0 & 0 & 0 & -1 & 0\\ 0 & 0 & 0 & 0 & 0 & -1\\ \mathcal{M}_{4,0}[\gamma] & \mathcal{M}_{4,1}[\gamma] & \mathcal{M}_{4,2}[\gamma] & \mathcal{M}_{4,3}[\gamma] & \mathcal{M}_{4,4}[\gamma] & \mathcal{M}_{4,5}[\gamma]\\ \mathcal{M}_{5,0}[\gamma] & \mathcal{M}_{5,1}[\gamma] & \mathcal{M}_{5,2}[\gamma] & \mathcal{M}_{5,3}[\gamma] & \mathcal{M}_{5,4}[\gamma] & \mathcal{M}_{5,5}[\gamma]\end{pmatrix} \times \begin{pmatrix}\mu_{b\gamma}(0)\\ \mu_{b\gamma}(1)\\ \mu_{b\gamma}(2)\\ \mu_{b\gamma}(3)\\ \mu_{b\gamma}(4)\\ \mu_{b\gamma}(5)\end{pmatrix} \tag{3.6}$$

(note, $\mathcal{M}_{4,0\leqslant j\leqslant 5} = -M_{E,b,\gamma}(6, j)$ and $\mathcal{M}_{5,0\leqslant j\leqslant 5} = -M_{E,b,\gamma}(7, j)$).

As indicated in the previous sections, given the starting values for the missing moments, $\{\mu_{b,\gamma=0}(i), (0 \leqslant i \leqslant 5)\}$, at any b, one can integrate the above equations. Facilitating the determination of these starting moment values is the relation in equation (2.6). Accordingly, one must determine the physical energy, E, and the physical missing moment values $\{\mu_{b=0,\gamma=0}(i), (0 \leqslant i \leqslant 5)\}$.

The $\mu_{0,0}(p)$ moments satisfy the moment equation

$$g\mu_{0,0}(p+6) = [E+\lambda(p+2)(p+1)]\mu_{0,0}(p) + \lambda E\mu_{0,0}(p+2) + p(p-1)\mu_{0,0}(p-2) \tag{3.7}$$

for $p \geqslant 0$. Symmetric configurations, such as the ground state, will have all their odd-order moments equal to zero, $\mu_{0,0}(\text{odd}) = 0$. For such configurations, one can streamline the formalism and work with the even-order Stieltjes moments $u(\rho) \equiv \mu_{0,0}(2\rho)$. Accordingly, only $u(0)$, $u(1)$, and $u(2)$ become the nonzero missing moments in this case. An analogous formulation is possible for antisymmetric configurations; however, for simplicity, these are not discussed in this paper.

The homogeneous nature of the moment equation requires some normalization condition. One convenient choice is

$$u(0) + u(1) + u(2) = 1. \tag{3.8}$$

Eliminating $u(0)$, all of the moments become linearly dependent on the unconstrained missing moments $u(1)$ and $u(2)$. This may be expressed through the relation $u(\rho) = \hat{M}_E(\rho, 0) + \sum_{j=1}^{2} \hat{M}_E(\rho, j)u(j)$, where the $\hat{M}_E$ coefficients are readily determinable from equation (3.4) and the above normalization.

The EMM quantization procedure involves making use of the positivity properties of the associated wavefunction in order to define constraints on the physically allowed energy and missing moment values. For the ground state wavefunction, the fact that $\Psi_{\text{ground}}(x) > 0$, allows us to impose the Hankel–Hadamard, nonlinear, determinental constraints on the E parameter and missing moment variables:

$$\Delta_{m,n}[E, u(1), u(2)] > 0 \qquad \text{for } m = 0, 1 \text{ and } n \geqslant 0 \tag{3.9a}$$

where

$$\Delta_{m,n} \equiv \mathrm{Det}\begin{pmatrix} u(m) & u(m+1) & \dots & u(m+n) \\ u(m+1) & u(m+2) & \dots & u(m+n+1) \\ \vdots & \vdots & \vdots & \vdots \\ u(m+n) & u(m+n+1) & \dots & u(m+2n) \end{pmatrix} \tag{3.9b}$$

and each of the Stieltjes moments, $u(\rho)$, is implicitly dependent on the energy parameter, E, and the unconstrained missing moments $u(1)$ and $u(2)$.

The algorithmic implementation of EMM theory is discussed in the works by Handy and Bessis (1985) and Handy *et al* (1988). It entails the use of linear programming (Chvatal 1983) to determine the E values admitting missing moment solution sets to the above inequalities. Implementation of this procedure for the ground state yields the ground-state energy and missing moment values (for $g = 1, \lambda = 0.1$):

$$E = 1.105\,005\,494\,535\,62$$
$$\mu_{0,0}(0) = 0.446\,117\,055\,534\,407$$
$$\mu_{0,0}(2) = 0.238\,142\,672\,555\,330$$
$$\mu_{0,0}(4) = 0.315\,740\,271\,910\,263$$
$$\mu_{0,0}(1,3,5) = 0.$$

Proceeding with a fourth-order Runge–Kutta numerical integration, we could only integrate out to an order $\gamma \approx 7$, before encountering numerical instability problems. However, even within this relatively small γ domain, the inverse γ expansion behaviour of $\mu_{b,\gamma}(p)$ was empirically satisfied for $\gamma \geqslant 4$. Specifically, from the integral representation in equation (2.3), upon performing the change of variable $y \equiv \sqrt{\gamma}x$ and Taylor expansion, at b, for $\Psi(b + \frac{y}{\sqrt{\gamma}})$, one obtains the expansion:

$$\mu_{b,\gamma}(p) = \gamma^{-\frac{(p+1)}{2}} \sum_{p+\rho=\text{even},\,\rho\geqslant 0}^{\infty} \frac{1}{\rho!}(\partial_b^\rho \Psi(b))\theta\left(\frac{p+\rho}{2}\right)\gamma^{-\frac{\rho}{2}} \tag{3.10}$$

where the θ coefficients are defined in the context of equation (2.9).

Consider fitting the Runge–Kutta iterates, $\mu_{b,\gamma_j}(p = 0, 2)$, for $J \leqslant j \leqslant J + N$, to a truncated analogue of the inverse γ expansion ($\rho =$ even, and $\rho \leqslant 2N$), for $4 \leqslant \gamma_j < 7$:

$$\mu_{b,\gamma_j}(p = \text{even}) = \gamma_j^{-\frac{(p+1)}{2}} \sum_{p+\rho=\text{even},\,\rho\geqslant 0}^{2N} \frac{1}{\rho!} C_J^{(p)}(b,\rho)\theta\left(\frac{p+\rho}{2}\right)\gamma_j^{-\frac{\rho}{2}}. \tag{3.11}$$

According to equation (2.9), the leading term of this expansion should approximate the wavefunction

$$C_J^{(p)}(b,0) \approx \Psi_{\text{exact}}(b). \tag{3.12}$$

Our numerical results confirm this. That is, a fourth-order Runge–Kutta integration directly on the Schrödinger equation, in order to obtain the exact ground-state wavefunction, normalized by $\Psi_{\text{exact}}(0) \equiv C_J^{(0,2)}(0,0)$, concurred with the truncated inverse γ expansion analysis $\Psi_{\text{exact}}(b) \approx C_J^{(0,2)}(b,0)$, for $|b| \leqslant 2.2$. The $C_J^{(0,2)}$ coefficient values given in figure 1 were generated at $\gamma = 4$. Also, although the Runge–Kutta $\delta\gamma$ step size was 10^{-5}, we generated the $C_J^{(0,2)}$ coefficients by sampling the Runge–Kutta iterates at intervals of $\gamma_{j+1} - \gamma_j = 10^{-1}$ (for $\gamma_j \approx 4$), to minimize round-off error fluctuations in inverting equation (3.11) to obtain the $C_J^{(0,2)}$s.

We used the inverse γ expansion to approximate the $\mu_{b,\gamma}(p)$ moments for $|b| \leqslant 2.2$ and $4 \leqslant \gamma < \infty$. This effectively accelerated the convergence of the direct numerical integration

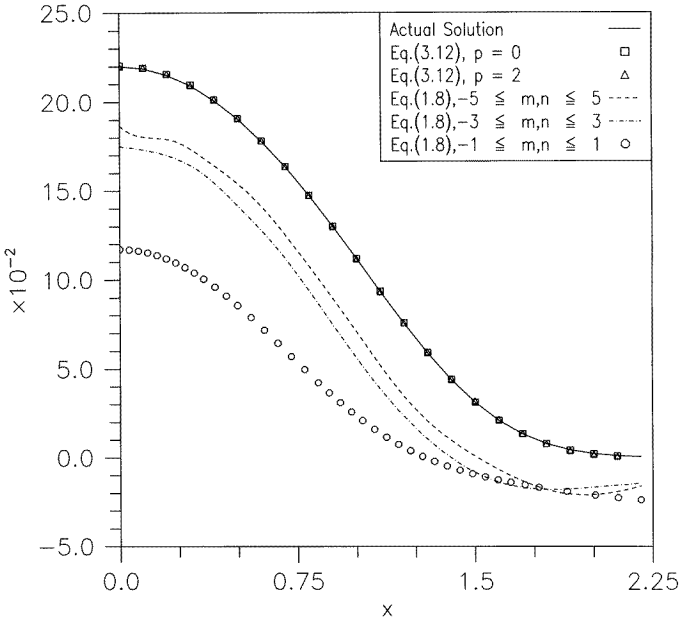

Figure 1. Ψ_{ground}, $V(x) = \frac{x^6}{1+.1x^2}$.

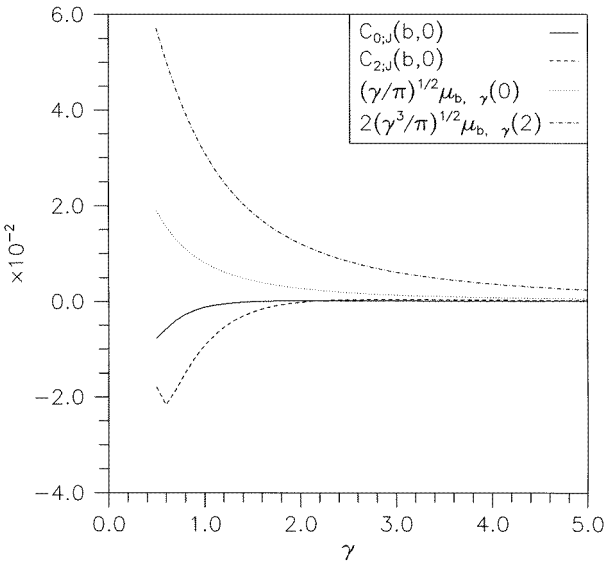

Figure 2. $\Psi(b)$ reconstruction at $b = +2.5$.

for the $\mu_{b,\gamma}(p)$ moments (refer to figures 2–7). Accordingly, the wavelet expansion coefficients $\omega_{m,n}$ are computable, in principle, for $|b = n2^m| \leqslant 2$ and $\gamma = \frac{1}{2(2^m)^2} =$ arbitrary. However, in practice we limit things to $|b = n2^m| \leqslant 2$ and $0 \leqslant \gamma < 7$.

In figure 1 we illustrate the exact ground-state solution, the asymptotic estimates achieved through the truncated inverse γ expansion ($N = 4$), and the wavelet reconstructed

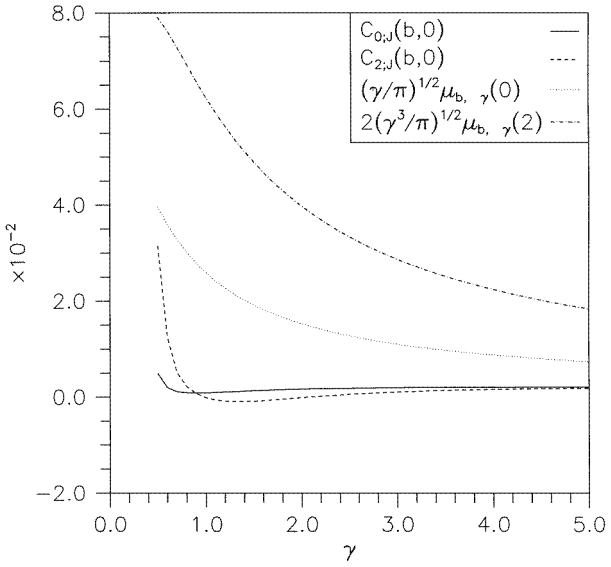

Figure 3. $\Psi(b)$ reconstruction at $b = +2.0$.

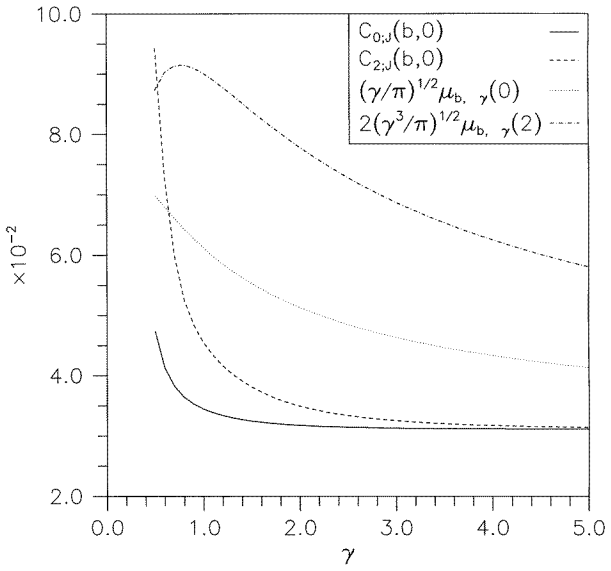

Figure 4. $\Psi(b)$ reconstruction at $b = +1.5$.

approximants. The results from the truncated inverse γ expansion are very good (equation (3.12)); whereas the wavelet reconstructed results are satisfactory.

It will be noted that the wavelet approximation in figure 1 appear to be off by a constant $\mathcal{C}$, within the depicted interval. One might speculate that this is due to our exclusion of terms (from equation (1.8)) corresponding to $n = 0$ and $a = 2^m \to \infty$, or $\gamma = \frac{1}{2^{2m+1}} \to 0$, making the argument of $\omega(\frac{(x-n2^m)}{2^m})$ very small (essentially, zero) for $|x| \leqslant 2$, the domain

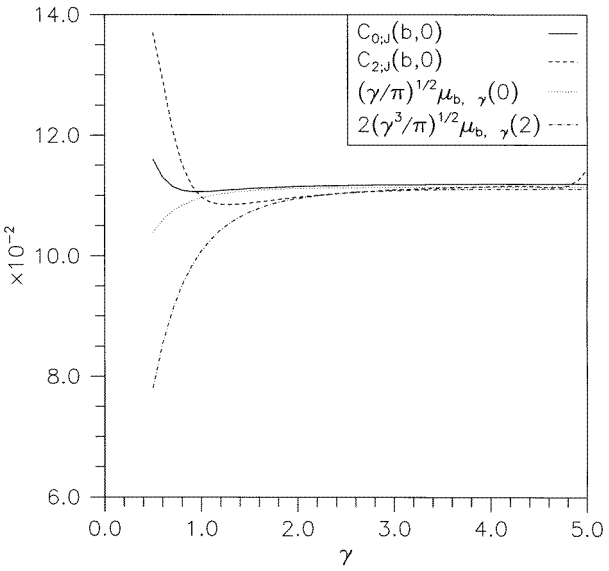

Figure 5. $\Psi(b)$ reconstruction at $b = +1.0$.

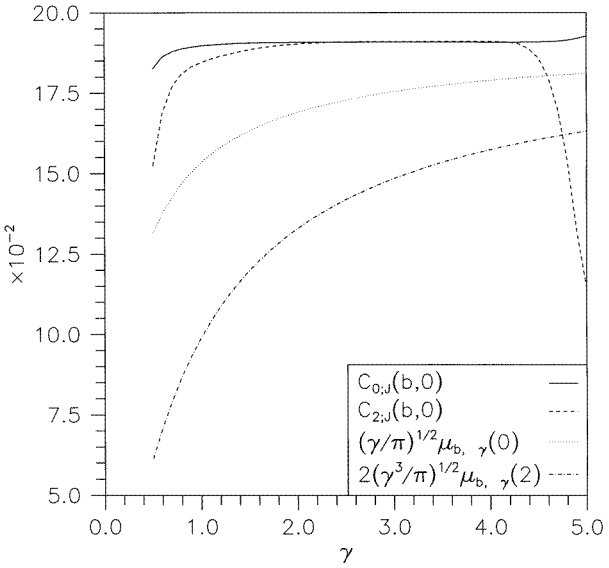

Figure 6. $\Psi(b)$ reconstruction at $b = +0.5$.

depicted in figure 1. We can estimate

$$\mathcal{C}_M = \frac{2}{A+B}\sum_{m=M}^{\infty}\omega_{m,0}\frac{1}{\sqrt{2^m}}\omega(0).$$

We have that (for the Mexican hat case)

$$\omega(0) = \mathcal{N} \equiv \frac{2}{\sqrt{3\sqrt{\pi}}} \qquad \text{and} \qquad \omega_{m,0} = W\Psi(2^m, 0) \approx \mathcal{N}\frac{1}{\sqrt{2^m}}\mu_{0,0}(0).$$

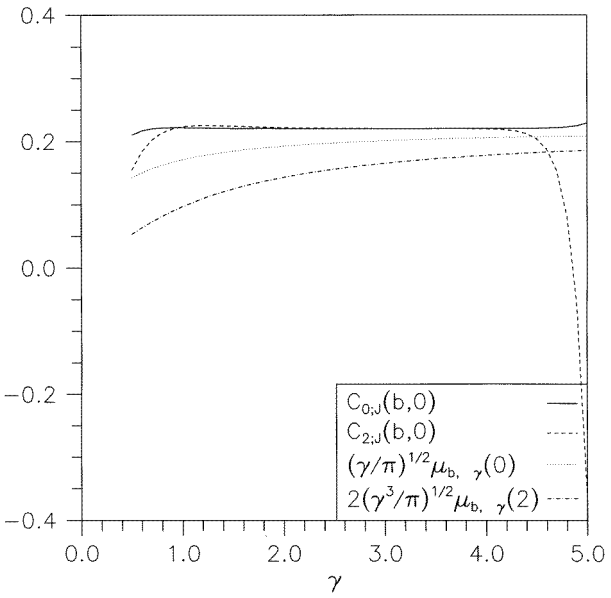

Figure 7. $\Psi(b)$ reconstruction at $b = 0.0$.

Putting it all together,

$$\mathcal{C}_M \approx \frac{4u(0)\mathcal{N}^2}{2^M(A+B)} = 0.44\frac{u(0)}{2^M}.$$

We then have that for the wavelet approximation corresponding to $-5 \leqslant m \leqslant 5$, $M = 6$, and $C_6 = 3 \times 10^{-3}$, which is off from the empirically determined constant $\mathcal{C}_{\text{empirical}} = 0.22 - 0.187 = 3 \times 10^{-2}$; therefore, additional significant corrections must come from the $n \neq 0$ terms as well.

In figures 2–7 we illustrate the γ dependence (b fixed) for $\sqrt{\frac{\gamma}{\pi}}\mu_{b,\gamma}(0)$, $2\sqrt{\frac{\gamma^3}{\pi}}\mu_{b,\gamma}(2)$, $C^{(0)}_{J_\gamma}(b,0)$, and $C^{(2)}_{J_\gamma}(b,0)$, where J_γ refers to the fact that these coefficients are obtained by fitting the (truncated) inverse γ expansion, at γ, to the $\mu_{b,\gamma}(0$ and $2)$ integrated results. Of course, as previously argued, all six of the curves in figures 2–7 must converge to $\Psi(b)$ (except for numerical instability problems).

We also show in figures 8–11 the wavelet-transform related expression $\frac{1}{\mathcal{F}}(2\gamma)^{\frac{5}{4}} W\Psi(\gamma, b)$ (for fixed γ values), where $\mathcal{F} \equiv \frac{2^{\frac{3}{2}}\pi^{\frac{1}{4}}}{\sqrt{3}}$. It can be easily argued that this expression must converge, pointwise, to $(E - V(b))\Psi(b)$, as $\gamma \to \infty$. Specifically, from equation (2.2) and equation (3.11), in the Mexican hat wavelet case,

$$\text{Lim}_{\gamma\to\infty}\, W\Psi(\gamma, b) = \mathcal{F}\left(\frac{1}{2\gamma}\right)^{\frac{5}{4}}(-\partial_b^2\Psi(b)) = \mathcal{F}\left(\frac{1}{2\gamma}\right)^{\frac{5}{4}}(E - V(b))\Psi(b).$$

The results illustrated in figures 8–11 confirm these asymptotic relations (the curve consisting of individual points is the function $[E - V(b)]\Psi_{\text{exact}}(b)$), except for the numerical *noise* appearing at $\gamma > \text{O}(10)$, for $b \approx 0$. Again, all the results shown for $\gamma > 4$ were obtained by using the truncated inverse γ expansion.

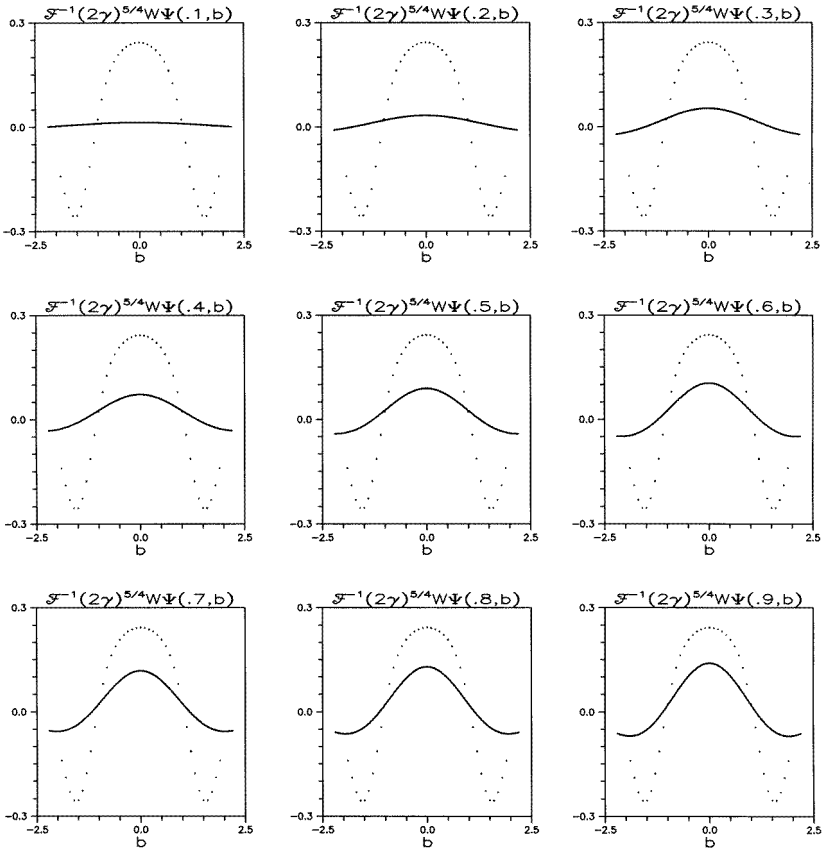

Figure 8. Verification of $\mathrm{Lim}_{\gamma\to\infty}\frac{(2\gamma)^{\frac{5}{4}}}{\mathcal{F}}W\Psi(\gamma,b)=(E-V(b))\Psi(b)$ (LHS denoted by full curve), $V(b)=\frac{b^6}{1+.1b^2}$, for various γ values.

4. The Coulomb potential

We consider the one-dimensional Coulomb problem defined by

$$-\partial_r^2\Psi(r)-\frac{1}{r}\Psi(r)=E\Psi(r) \tag{4.1}$$

where $\Psi(0)=0$. The wavelet transform, for the Mexican hat case, is

$$W\Psi(\gamma,b)=\mathcal{N}(2\gamma)^{\frac{1}{4}}\int_0^\infty \mathrm{d}r\,(1-2\gamma(r-b)^2)\exp(-\gamma(r-b)^2)\Psi(r) \tag{4.2}$$

or

$$W\Psi(\gamma,b)=\mathcal{N}(2\gamma)^{\frac{1}{4}}[(1-2b^2\gamma)\mu_{b,\gamma}(0)+4b\gamma\mu_{b,\gamma}(1)-2\gamma\mu_{b,\gamma}(2)] \tag{4.3}$$

where

$$\mu_{b,\gamma}(p)\equiv\int_0^\infty \mathrm{d}r\,r^p\exp(-\gamma(r-b)^2)\Psi(r). \tag{4.4}$$

The differential equation for $\Phi_{b,\gamma}(r)\equiv\exp(-\gamma(r-b)^2)\Psi(r)$ is

$$-[\partial_r^2+4\gamma(r-b)\partial_r+(2\gamma+4\gamma^2(r-b)^2)]\Phi_{b,\gamma}-\frac{1}{r}\Phi_{b,\gamma}(r)=E\Phi_{b,\gamma}(r). \tag{4.5}$$

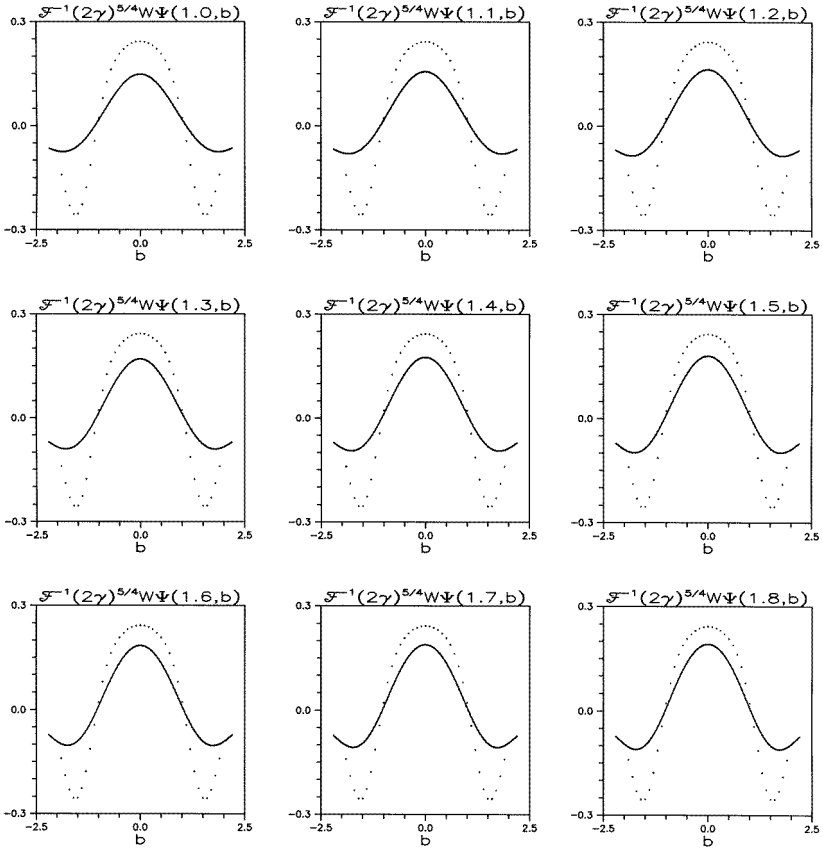

Figure 9. $\mathrm{Lim}_{\gamma\to\infty}\frac{(2\gamma)^{\frac{5}{4}}}{\mathcal{F}}W\Psi(\gamma,b)=(E-V(b))\Psi(b)$, $1\leqslant\gamma\leqslant 1.8$.

Multiplying both sides by r^{1+p}, integrating from 0 to ∞, and performing the necessary integration by parts (recalling that $\Phi_{b,\gamma}(0)=0$) yields the moment equation:

$$4\gamma^2\mu_{b,\gamma}(p+3)=-p(p+1)\mu_{b,\gamma}(p-1)-[4b\gamma(p+1)+1]\mu_{b,\gamma}(p)$$
$$+[4\gamma(p+2)-2\gamma-E-4\gamma^2b^2]\mu_{b,\gamma}(p+1)+8\gamma^2b\mu_{b,\gamma}(p+2). \qquad (4.6)$$

It is important to appreciate the significance of such moment equations. The potential, $V(r)$, determines the asymptotic behaviour of the physical and unphysical states, $\Psi(r)\to\exp(\pm\int\sqrt{V(r)-E})$, from the usual JWKB analysis (Bender and Orszag 1978). In the case that one is considering generalized moments of the type in equation (4.4), such moments cannot exist if the unphysical solution grows faster than the Gaussian exponential drop-off. Nevertheless, the above moment equation, in general, can be made to yield finite moments even for unphysical values of the energy. A simple case is the previous $\frac{x^6}{1+0.1x^2}$ problem. In the present case of the Coulomb problem, the Gaussian kernel dominates the $\exp(+\sqrt{-E}r)$ asymptotic behaviour for unphysical states. As such, the moment equation would yield their generalized moments.

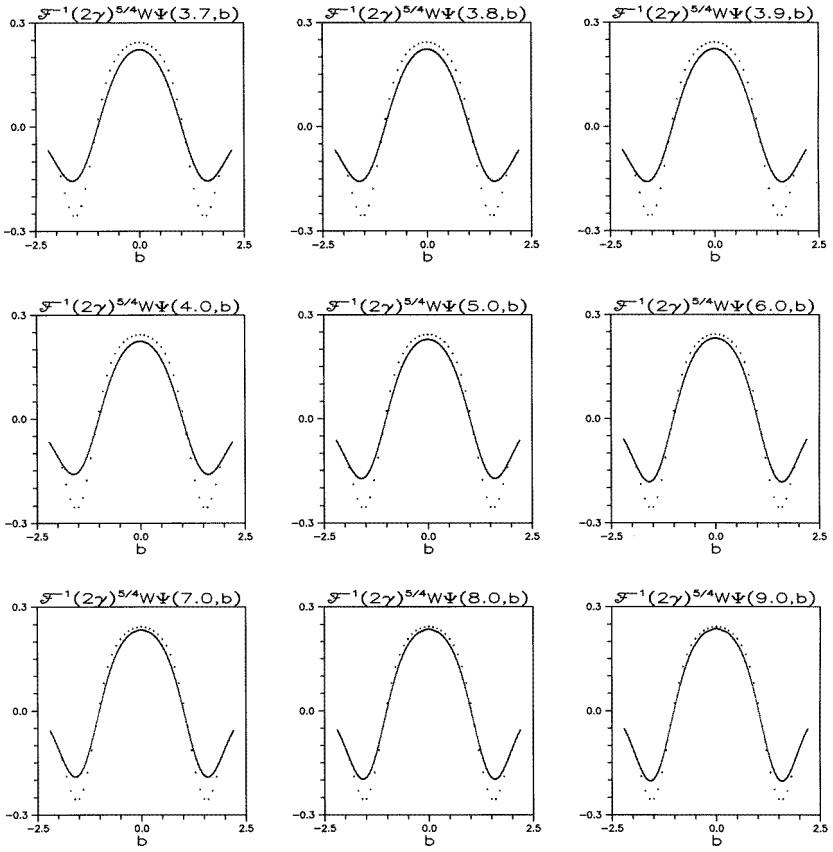

Figure 10. $\mathrm{Lim}_{\gamma\to\infty}\frac{(2\gamma)^{\frac{5}{4}}}{\mathcal{F}}W\Psi(\gamma,b)=(E-V(b))\Psi(b)$, $3.7\leqslant\gamma\leqslant 9$.

The moment equation involves three missing moments $\{\mu_{b,\gamma}(i)|0\leqslant i\leqslant 2\}$, so long as $\gamma\neq 0$; therefore,

$$\mu_{b,\gamma}(p)=\sum_{i=0}^{2}M_{E,b,\gamma}(p,i)\mu_{b,\gamma}(i)\qquad\text{for } 0\leqslant i\leqslant 2. \tag{4.7}$$

From equation (4.4), we have that

$$\partial_\gamma\mu_{b,\gamma}(p)=-\mu_{b,\gamma}(p+2)+2b\mu_{b,\gamma}(p+1)-b^2\mu_{b,\gamma}(p). \tag{4.8}$$

With respect to the missing moments, we obtain

$$\frac{\partial}{\partial\gamma}\begin{pmatrix}\mu_{b,\gamma}(0)\\ \mu_{b,\gamma}(1)\\ \mu_{b,\gamma}(2)\end{pmatrix}=\begin{pmatrix}-b^2 & 2b & -1\\ \left(\frac{b}{\gamma}+\frac{1}{4\gamma^2}\right) & \left(\frac{E}{4\gamma^2}-\frac{3}{2\gamma}\right) & 0\\ \frac{1}{2\gamma^2} & \left(\frac{2b}{\gamma}+\frac{1}{4\gamma^2}\right) & \left(\frac{E}{4\gamma^2}-\frac{5}{2\gamma}\right)\end{pmatrix}\begin{pmatrix}\mu_{b,\gamma}(0)\\ \mu_{b,\gamma}(1)\\ \mu_{b,\gamma}(2)\end{pmatrix}. \tag{4.9}$$

The singular nature of these equations complicates its numerical γ-integration starting from the origin $\gamma=0$. The moments are not analytic at $\gamma=0$ because the moment integral in equation (4.4) is divergent for negative γ values due to the pure exponential drop-off nature of the physical states ($\mathrm{Lim}_{r\to\infty}\Psi(r)=r\exp(-\sqrt{|E|}r)$).

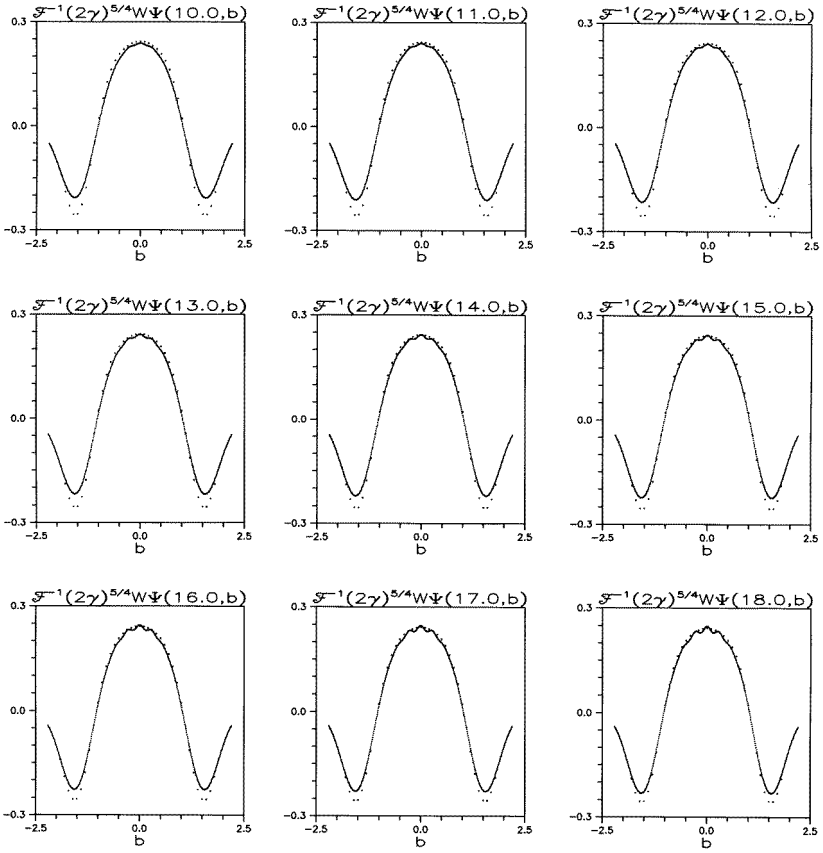

Figure 11. $\mathrm{Lim}_{\gamma\to\infty}\frac{(2\gamma)^{\frac{5}{4}}}{\mathcal{F}}W\Psi(\gamma,b)=(E-V(b))\Psi(b)$, $10\leqslant\gamma\leqslant 18$.

In order to be able to integrate equation (4.9), we must be able to solve for the moments at some $\gamma\neq 0$ value (and all b values) and then integrate in both directions: zero and infinity. We will designate the chosen starting γ value by γ_s.

It will be noted that $\mu_{b,\gamma=0}(p)=\mu_{0,0}(p)$. The $u(p)\equiv\mu_{0,0}(p)$ moments, as well as the energy, E, can be obtained from the EMM method (Handy and Bessis 1985). One important observation is that the $\gamma=0$ case corresponds to a zero missing moment problem in which the normalization prescription can be taken to be $u(0)=1$. More precisely, if we set $\gamma=0$ in equation (4.6), the ensuing moment equation involves no missing moments once we set $u(0)=\mu_{0,0}(0)=1$. The EMM method works very well for the zero missing moment problem ($\gamma=0$). For problems in which the unphysical states become asymptotically unbounded (at least in one direction) much faster than the $\exp(-\gamma r^2)$ kernel in equation (4.4), ensuring that the moments for $\Phi_{\text{unphysical}}$ do not exist, then EMM is applicable and will yield converging bounds to the discrete-state energy and missing moments. When this is not satisfied, then EMM cannot be made to yield converging bounds for the energy and missing moments. However, if the energy is known *a priori*, which it is in this case (since we can use EMM for the zero missing moment problem corresponding to $\gamma=0$), then we can use EMM to yield good estimates for the missing moments, $(\mu_{b,\gamma_s}(0),\mu_{b,\gamma_s}(1),\mu_{b,\gamma_s}(2))$.

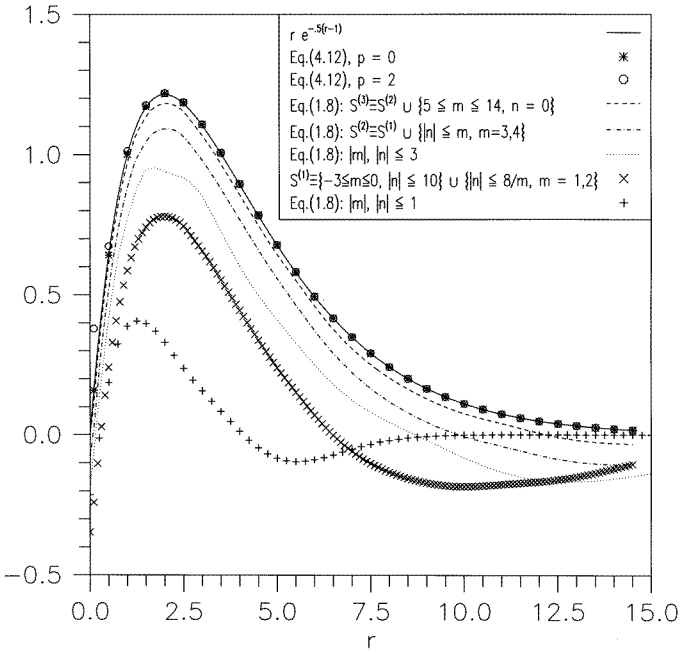

Figure 12. Wavelet reconstruction for the Bohr ground state, $r\exp(-\frac{1}{2}[r-1])$. The selection of the set $S^{(1)}$ (together with equation (1.8)) is motivated by consideration of the more important wavelet coefficients consistent with the numerical integration domain studied: $\frac{1}{2\times 4^2} \leqslant \gamma \leqslant \frac{1}{2\times 4^{-3}}$, or $-3 \leqslant m \leqslant 2$. Improvement in the wavelet reconstructed approximation (data corresponding to $S^{(2)}$ and $S^{(3)}$) is obtained by looking at additional wavelet coefficients, for $m \geqslant 3$, computed using *Mathematica*.

One must be careful in using EMM to determine $\{\mu_{b,\gamma_s}(0-2)\}$, since for each b value an implicitly varying normalization prescription is used, $\sum_{i=0}^{2}\mu_{b,\gamma_s}(i) = 1$. In order to ensure that the underlying wavefunction, $\Psi(r)$, has a fixed normalization, we can only use EMM at one particular b value (say, $b = 0$), and then integrate along the b-direction to obtain the other missing moment values. To do this, we must make use of the relation (from equation (4.4))

$$\partial_b \mu_{b,\gamma}(p) = 2\gamma[\mu_{b,\gamma}(p+1) - b\mu_{b,\gamma}(p)]. \tag{4.10}$$

For the missing moments, this becomes:

$$\frac{\partial}{\partial b}\begin{pmatrix}\mu_{b,\gamma}(0)\\ \mu_{b,\gamma}(1)\\ \mu_{b,\gamma}(2)\end{pmatrix} = \begin{pmatrix} -2b\gamma & 2\gamma & 0\\ 0 & -2b\gamma & 2\gamma\\ -\left[2b+\dfrac{1}{2\gamma}\right] & \left[3-\dfrac{E}{2\gamma}-2\gamma b^2\right] & 2b\gamma\end{pmatrix}\begin{pmatrix}\mu_{b,\gamma}(0)\\ \mu_{b,\gamma}(1)\\ \mu_{b,\gamma}(2)\end{pmatrix}. \tag{4.11}$$

We used EMM to determine the moments at $b = 0$ and $\gamma_s = 0.05$. The (approximate) values are $\mu_{0,0.05}(0) = 0.087\,999\,2498$, $\mu_{0,0.05}(1) = 0.211\,996\,0726$, $\mu_{0,0.05}(2) = 0.700\,004\,6776$. We can easily integrate equation (4.11) from $b = 0$ to $b = 15$, and higher. Utilizing the generated values $\{\mu_{b,0.05}(0-2)|0 \leqslant b \leqslant 15\}$, we can then use equation (4.9) to integrate in the γ direction. We did so for $\gamma \to 100$. The asymptotic relations (resulting

Table 1. $\Psi(b < 0)$ Estimates from equation (4.12).

b	γ	$\sqrt{\frac{\gamma}{\pi}}\mu_{b,\gamma}(0)$	$\sqrt{\frac{\gamma}{\pi}}b^{-2}\mu_{b,\gamma}(2)$
−0.5	100	0.502(−3)[a]	0.500(−3)
−1.0	100	0.341(−3)	0.340(−3)
−1.5	100	0.245(−3)	0.244(−3)
−2.0	100	0.178(−3)	0.178(−3)
−2.5	100	0.130(−3)	0.130(−3)
−3.0	100	0.939(−4)	0.937(−4)
−3.5	100	0.671(−4)	0.669(−4)
−4.0	100	0.472(−4)	0.471(−4)
−4.5	100	0.327(−4)	0.326(−4)
−5.0	100	0.222(−4)	0.222(−4)
−5.5	100	0.148(−4)	0.148(−4)
−6.0	100	0.966(−5)	0.965(−5)
−6.5	100	0.616(−5)	0.615(−5)
−7.0	100	0.382(−5)	0.381(−5)
−7.5	100	0.227(−5)	0.227(−5)
−8.0	100	0.127(−5)	0.127(−5)
−8.5	100	0.609(−6)	0.608(−6)
−9.0	100	0.160(−6)	0.159(−6)
−9.5	100	−0.173(−6)	−0.173(−6)
−10.0	100	−0.455(−6)	−0.455(−6)
−10.5	100	−0.737(−6)	−0.737(−6)
−11.0	100	−0.106(−5)	−0.106(−5)
−11.5	100	−0.146(−5)	−0.146(−5)
−12.0	100	−0.197(−5)	−0.197(−5)
−12.5	100	−0.264(−5)	−0.264(−5)
−13.0	100	−0.353(−5)	−0.354(−5)
−13.5	100	−0.471(−5)	−0.472(−5)
−14.0	100	−0.628(−5)	−0.628(−5)
−14.5	100	−0.833(−5)	−0.835(−5)

[a] Denotes power of 10.

from the fact that $\sqrt{\frac{\gamma}{\pi}}\exp(-\gamma(r-b)^2) \to \delta(r-b)$, as $\gamma \to \infty$)

$$\mathrm{Lim}_{\gamma\to\infty}\sqrt{\frac{\gamma}{\pi}}\mu_{b,\gamma}(p) = b^p\Psi(b) \tag{4.12}$$

was readily confirmed ($p = 0, 2$) and used to generate the ground-state solution (normalized according to $\sum_{i=0}^{2}\mu_{0,0.05}(i) = 1$). In order to compare the results with the true answer (normalized to unity at $r = 1$), $\Psi_{\mathrm{gr.}}(r) = r\exp(-\frac{1}{2}(r-1))$, we had to renormalize our integration results according to $N(\Psi(1) = \sqrt{\frac{\infty}{\pi}}\mu_{b=1,\infty}(0)) = 1$. The results were consistently accurate within less than 1%, for $0 \leqslant b \leqslant 15$. This is depicted in figure 12.

For unphysical r values ($r < 0$), all the above can be implemented. Consistent with the implicit assumption from equation (4.4) that $\Psi(r < 0) = 0$, the above numerical integration yields $\Psi_{\mathrm{approx}}(r < 0) \approx 0$ (specifically, values of the order of $\mathrm{O}(10^{-3})$ to $\mathrm{O}(10^{-6})$ as noted in table 1).

In order to compare the above results with those coming from a wavelet reconstruction ansatz (utilizing equation (1.8)), it is empirically important to consider the contribution from $\gamma_s < 0.05$. In order to integrate in this regime, we must perform a change of variables for

equation (4.9) involving $\alpha = \frac{1}{2\gamma} = a^2$. We obtain:

$$\frac{\partial}{\partial\alpha}\begin{pmatrix}\mu_{b,\alpha}(0)\\ \mu_{b,\alpha}(1)\\ \mu_{b,\alpha}(2)\end{pmatrix} = \begin{pmatrix} \dfrac{b^2}{2\alpha^2} & -\dfrac{b}{\alpha^2} & \dfrac{1}{2\alpha^2} \\ -\left(\dfrac{b}{\alpha}+\dfrac{1}{2}\right) & -\left(\dfrac{E}{2}-\dfrac{3}{2\alpha}\right) & 0 \\ -1 & -\left(\dfrac{2b}{\alpha}+\dfrac{1}{2}\right) & -\left(\dfrac{E}{2}-\dfrac{5}{2\alpha}\right)\end{pmatrix}\begin{pmatrix}\mu_{b,\alpha}(0)\\ \mu_{b,\alpha}(1)\\ \mu_{b,\alpha}(2)\end{pmatrix}. \quad (4.13)$$

Utilizing the initial values quoted above ($\mu_{b,\gamma}(p)$, for $0 \leqslant b \leqslant 15$, $\gamma = 0.05$, *and* $0 \leqslant p \leqslant 2$), we can integrate equation (4.13) from $\alpha_s = \frac{1}{2\times 0.05} = 10$ up to a sufficiently large α value at which point an asymptotic expansion of the moment integrals will be applicable for $\alpha \to \infty$. Specifically (Abramowitz and Stegun 1972), from equation (4.4):

$$\mu_{b,\gamma=\frac{1}{2\alpha}}(p) = \exp(-\gamma b^2)\sum_{\rho=0}^{\infty}\gamma^{\rho}\sum_{\rho_1+\rho_2=\rho}\frac{(-1)^{\rho_1}(2b)^{\rho_1}}{\rho_1!\rho_2!}\mu_{0,0}(p+2\rho_1+\rho_2). \quad (4.14)$$

By implementing an appropriate *asymptotic matching* procedure (Bender and Orszag 1978) with the integrated results from equation (4.13), we can recover the $\mu_{0,0}(p)$ moments corresponding to the adopted normalization used in generating the missing moments at $b = 0$, $\gamma = 0.05$ ($\sum_{i=0}^{2}\mu_{0,0.05}(i) = 1$). For the purposes of this 'pedagogic' analysis, we used the exact values instead, $\mu_{0,0}(p) = \exp(\frac{1}{2})2^{p+2}(p+1)!$, corresponding to the normalization depicted in figure 12. Specifically, we were able to use equation (4.14) to integrate up to $\gamma = \frac{1}{2\times 4^3} = 0.007\,8125$, for $b = 0$, and $\gamma = \frac{1}{2\times 4^2} = 0.031\,25$, for larger $b \approx \mathrm{O}(10)$ values. Since the ground-state wavefunction is known (and in particular $\mu_{b,\gamma}(0)$ is easily related to the $Erfc(z)$ function (Abramowitz and Stegun 1972)) one can readily use *Mathematica* to generate many of the more important wavelet coefficients $\omega_{m,n}$ (from equation (1.8)) corresponding to small γ values ($\gamma = \frac{1}{2\times 4^m}$, $m \geqslant 3$).

The results in figure 12 yield an impressive confirmation of the validity of equation (1.8). To obtain the illustrated results, we utilized our formalism to obtain the wavelet coefficients corresponding to $|b = n2^m| \leqslant 16$ (from equation (4.9)), as well as $\omega_{(m=2,n)}$, for $|n| \leqslant 4$ (from equation (4.13)). Simply using these coefficients only gave the poorer curves depicted in figure 12; including the wavelet coefficients for $\omega_{(m,n=0)}$, where $m \leqslant 20$, did substantially improve things. Upon adding more coefficients (generated from *Mathematica*) corresponding to small γ values and $|b| \leqslant 32$, better results were obtained. In all, 155 wavelet coefficients were used.

The wavelet reconstruction results for $b < 0$ yielded an oscillatory configuration with absolute magnitude of order $\mathrm{O}(10^{-1})$ (based on the same 155 wavelet coefficients) and illustrated in figure 13. It is compared with the results presented in table 1. Note that in figure 13, the data corresponding to $p = 0$ and $p = 2$ appear to coincide, due to their inherent accuracy (refer to table 1) and the resolution available in the illustration.

5. Conclusion

We have shown that a moment-based formalism enables the generation of the wavelet transform for one-dimensional rational potential problems, from first principles, without any theoretical approximations. The recovery (reconstruction) of the discrete-state wavefunction is then possible through two approaches. The first involves the use of asymptotic moment relations of the type given in equation (2.9). The second makes use of the dyadic wavelet reconstruction approximation, as represented in equation (1.8). The first procedure gives excellent results; whereas the dyadic-reconstruction-based approximants appear to slowly

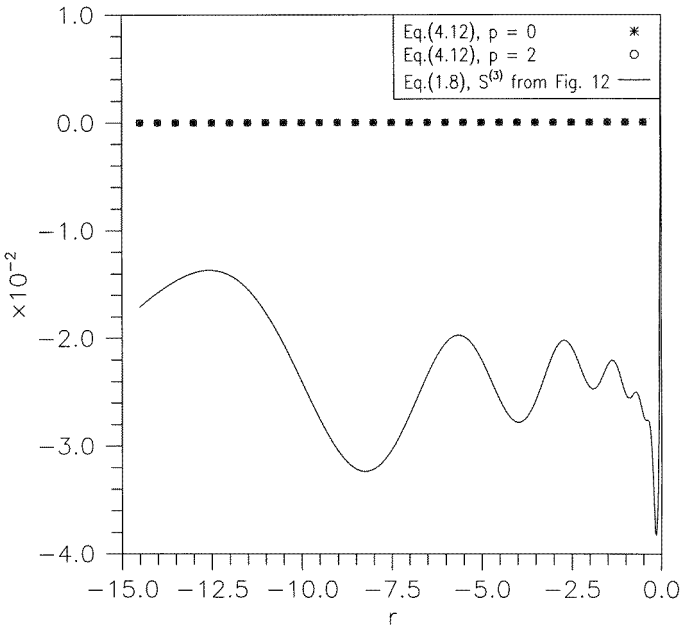

Figure 13. Wavelet reconstruction in the unphysical region ($r < 0$) for Bohr ground state, $\Psi(r < 0) \equiv 0$. Isolated points correspond to limit in equation (4.12) (also given in table 1); continuous curve corresponds to dyadic wavelet reconstruction formula in equation (1.8).

converge to the true solution. Nevertheless, for the one-dimensional Coulomb potential, the dyadic reconstruction yields very good results, provided a large number of terms are generated. Despite the manifest dichotomy in reconstruction procedures, in fact they are both wavelet based. Specifically, we can show that the asymptotic relation in equation (2.9) is exactly a wavelet-transform based result, corresponding to the integration over all scales $0 \leqslant a < \infty$ and translation parameter values $-\infty < b < +\infty$. The details of this will be presented elsewhere (Handy and Murenzi 1997).

Acknowledgments

This work was supported in part by the National Science Foundation through the Center for Theoretical Studies of Physical Systems and HRD 9450380 and is an outgrowth of initial support and encouragement from NAWC-Chinalake and Mr Harold Brooks. Partial support from ONR grant N00014-93-1-0561 is acknowledged. We would like to thank Professor Jean-Pierre Antoine, Professor Ingrid Daubechies, Professor Giorgio Mantica, Professor Alfred Msezane, Professor C J Tymczak, Professor Xiao Qian Wang and Professor Guido Weiss for useful discussions.

References

Abramowitz M and Stegun I A (ed) 1972 *Handbook of Mathematical Functions* (New York: Dover)

Bender C M and Orszag S A 1978 *Advanced Mathematical Methods for Scientists and Engineers* (New York: McGraw-Hill)

Blankenbecler R, De Grand T and Sugar R L 1980 *Phys. Rev.* D **21** 1055

Chvatal V 1983 *Linear Programming* (New York: Freeman)

Cho K, Arias T A, Joannopoulos J D and Lam P K 1993 *Phys. Rev. Lett.* **71** 1808
Chui C K 1992 *An Introduction to Wavelets* (New York: Academic)
Daubechies I 1990 *IEEE Trans. Inform. Theor.* **36** 961
——1991 *Advances in Spectrum Analysis and Array Processing* vol I, ed S Haykin (Englewood Cliffs, NJ: Prentice-Hall)
——1992 *Ten Lectures on Wavelets* (Philadelphia, PA: SIAM)
Daubechies I, Grossmann A and Meyer Y 1986 *J. Math. Phys.* **27** 1271
Duffin R J and Schaefer A C 1952 *Trans. Am. Math. Soc.* **72** 341
Fernandez F M and Ogilvie J F 1993 *Phys. Lett.* A **178** 11
Frazier M, Jawerth B and Weiss G 1988 The ϕ-transform and applications to distribution spaces *Function Spaces and Application (Lecture Notes in Mathematics 1302)* ed M Cwikel (Berlin: Springer) pp 233–46
Grossmann A and Morlet J 1984 *SIAM J. Math. Anal.* **15** 723
Handy C R 1996 *J. Phys. A: Math. Gen.* **29** 4093
Handy C R and Bessis D 1985 *Phys. Rev. Lett.* **55** 931
Handy C R, Bessis D, Sigismondi G and Morley T D 1988 *Phys. Rev. Lett.* **60** 253
Handy C R and Lee P 1991 *J. Phys. A: Math. Gen.* **24** 1565
Handy C R and Murenzi R 1996 *Phys. Rev.* A **54** 3754
——1997 *Proc. 1996 Montreal Workshop on Spline Functions and the Theory of Wavelets*
Killingbeck J P, Jones M N and Thompson M J 1985 *J. Phys. A: Math. Gen.* **18** 793
Paul T 1984 *J. Math. Phys.* **25** 3252
Plantevin F 1992 Une application de la transformée en ondelettes continue à la mécanique quantique et analyse multi-résolution adaptive *PhD Thesis* Université de Provence, France
Shohat J A and Tamarkin J D 1963 *The Problem of Moments* (Providence, RI: American Mathematical Society)
Witwit M R M 1995 *J. Math. Phys.* **36** 187